Drew University

College of Liberal Arts

**Mapping Odor Representation in the
Olfactory Tubercle and Superficial Amygdaloid Nuclei**

A Thesis in Neuroscience

by

Kyla Moutenot

Submitted in Fulfillment

of the Requirements

for the Degree of

Bachelor in Arts

With Specialized Honors in Neuroscience

May 2018

Abstract

      The representation of odor stimuli across olfactory structures is poorly understood. The objectives of this study were to characterize features of odor processing in two primary olfactory regions - olfactory tubercle and amygdala - by describing odor responsivity, tuning breadth, and correlated tuning of adjacent neurons. This study compiled and analyzed data collected by previous students in the Cousens laboratory at Drew University consisting of electrophysiological recordings of neuronal response profiles to different sets of monomolecular odorants and pheromones. Across 31 recording sessions in 16 rat subjects, 35 tubercle neurons and 33 amygdala neurons were analyzed. Odor-responsive neurons were isolated in tubercle and amygdala. Both regions responded similarly to each other when presented with different monomolecular odors, and different monomolecular odors produced different responses in both regions. There were no significant differences in tubercle neuron responses to monomolecular odors compared to pheromones. Pheromones were not presented to amygdala neurons. Tubercle and amygdala neurons both demonstrated broad tuning breadths in response to monomolecular odorants. In response to the least-preferred odors, tubercle neurons were more selective and responded less than amygdala neurons. Only four tubercle cell pairs demonstrated significant correlated tuning; no amygdala cell pairs were significant. Four additional tubercle cell pairs and one amygdala cell pair were considered correlated with visual evaluation of histograms. These results may be explained by innervation from olfactory bulb projections and the procedures used to collect data. Together, these results describe response profiles of neurons in tubercle and amygdala and suggest both regions

play an important role in olfactory processing. This ultimately sets the stage for further analysis of manipulation of olfactory system networks in brain regions that are continually being explored.

Table of Contents

Title Page
Abstract
Table of Contents
Thesis Chapters

Introduction

Throughout all stages of life, organisms exhibit survival behaviors. Newborn rat pups clumped together to reduce heat loss and avoid homeostatic imbalance while adult rats exhibited parental behaviors towards rat pups from a different mother (Alberts, 1978; Rosenblatt, 1967). More specifically, olfaction is a primitive survival mechanism used across all ages of development in animals. Odor processing helped animals understand their external environment in multiple ways, such as finding food, identifying mates, and engaging in intraspecific and interspecific communication (Axel, 1995).

Olfaction may be specifically involved in evaluating how dangerous a situation is. The primary predators of rodents were carnivores such as cats, dogs, wolves, and foxes. Trimethylthiazoline (TMT), a component of fox feces, was presented to naive rat subjects in a controlled setting to mimic the presence of a predator (Fendt et al., 2005). Subjects were bred in a laboratory and had never been exposed to natural predators, yet interestingly, still anticipated danger after detecting predator odors. This validated that olfactory processing played a role in fearful behavioral responses (Fendt et al., 2005).

In neocortical sensory areas, neurons that are responsive to similar features of stimuli tended to be spatially clustered together in a way that allows for response profiles to vary smoothly across a cortex (Stettler and Axel, 2009). However, this was not demonstrated by the olfactory system and should be further investigated to better understand sensory processing. Subsequent paragraphs will discuss common features demonstrated by other sensory systems, pinpoint features of the olfactory system that differ, and investigate the representation of odors across the cortical space of two primary

olfactory regions which receive direct input from the olfactory bulb – the olfactory tubercle (OT) and amygdala (AMG) – and make comparisons to an olfactory structure that also receives direct innervation from the olfactory bulb: a structure known as piriform cortex (Pir).

Organization of Non-Olfactory Primary Sensory Cortices

When a stimulus is presented, sensory information is transmitted to the brain to be further processed, with the final goal of eliciting an appropriate behavioral response (Sosulski et al., 2011). Although we have multiple senses, our sensory systems share some common features; these features include organization into layers and/or columns, where cortical layers have different functions depending on target output, and neurons in one column are likely to have similar functions to adjacent columns, with similarity in function decreasing with distance between columns. Most sensory systems also demonstrate topography, meaning that cells with similar preferences in stimulus features gradually and smoothly vary across cortical space (Mountcastle, 1997). These features are depicted in Figure 1.

<INSERT FIGURE 1>

The neocortex consists of the outer layer of the cerebrum and is known for higher functions such as sensory perception, spatial reasoning, generation of motor commands, and consciousness. This cortex is organized into vertical columns and six layers, shown in Figure 1a. Each column represents an individual unit. Units similar in function are close in proximity because overlapping internal processing chains allow for short-distance distribution of information across columns. Shown in Figure 1a by different

shades of gray, a columnar organization creates a gradual representation of sensory information across cortical space in the neocortex (Mountcastle, 1997). On the other hand, layers are segregated by output target structure. While layers I -III have horizontal projections to other cortical regions, layer IV communicates with the thalamus – a structure that processes various types of sensory input and relays this information to subsequent structures in each sensory pathway – and layers V and VI project to subcortical structures. This organization results in different cell types across each cortical layer of the neocortex, represented by different cell morphologies in Figure 1a (Mountcastle, 1997; Tyll et al., 2011).

Similarly, neurons located in the medial occipital lobe in the primary visual cortex (V1) process visual input within columns and across cortical space (Figure 1b). V1 neurons are orientation-selective, meaning they are more responsive to - or have a preference for - a certain orientation of a beam of light (Tootell et al., 1998). This organization causes V1 neurons to have the same orientation preference with vertical advancement down a column. V1 neurons respond to orientations of light similar to neurons in adjacent columns, shown by the gradual change in orientation preference with advancement across cortical space in Figure 1b. This continuous transition in preference ultimately creates orientation columns circling around a center point in the shape of a pinwheel, shown in Figure 1b with different colors representing different orientation preferences (Bonhoeffer and Grinvald, 1991). In addition to orientation columns, V1 displays a more specific type of topography called retinotopy. When different patterns of

stimuli are presented, the image detected by the retina is mapped across V1 cortical surface with roughly the same proportions as the original stimulus (Tootell et al., 1998).

The primary auditory cortex (A1) is involved in the perception of sound. The cochlea is a structure located in the inner ear that plays a role in processing frequency of auditory stimuli. The cochlea responds to lower frequencies at its apex, and responds to higher frequencies with gradual advancement towards its base (Reale, 1979). The integrity of this orderly frequency gradient is preserved in the cat A1, shown in Figure 1c. Lower frequencies are processed in the rostral portion of A1 while higher frequencies are processed in the caudal portion, with an increasing progression in the frequency when advancing caudally. However, the basal cochlea is more largely represented in caudal A1 relative to how the apex of the cochlea is represented in rostral A1; this may be explained by the need for more neural mechanisms for processing higher frequencies (Merzenich et al., 1974; Reale, 1979). This disproportional representation does not mimic the proportional representation of visual stimuli in V1, but overall, the stepwise frequency preference demonstrated in A1 can be held analogous to the gradual change in similar types of sensory information across columns in the neocortex as well as the gradual change in orientation preference across columns in the visual system (Merzenich et al., 1974).

Although several sensory systems organize input across columns and layers using a topographical layout modified to the type of sensory information being processed, these are not the only ways that input can be represented in the brain. In fact, the olfactory system differs in its organization of olfactory input.

The Olfactory System

      Unlike the layout of other sensory systems, the olfactory system does not demonstrate topography across each of its structures. Subsequent paragraphs discuss how olfactory input is processed, how different primary olfactory structures represent olfactory input in different ways, and how the OT and the regions of AMG that receive olfactory input are relevant to the overall processing of olfactory information. The odor-processing pathway from the detection of odors in the nares through the primary olfactory structures is depicted in Figure 2.

<INSERT FIGURE 2>

      When an animal inhales, odorant molecules bind to and are detected by olfactory receptor neurons (ORNs) on cilia that protrude out of the olfactory epithelium in the nares (Figure 2). More than 1,000 different receptors can be expressed across the olfactory epithelium. Shown in Figure 2, sensory information is then transmitted to the olfactory bulb (OB) – the first processing site of olfactory information in the brain (Axel, 1995). Axons extending from olfactory receptor neurons converge onto a singular OB glomerulus, a cluster of nerve endings. An individual glomerulus receives input from olfactory receptor neurons that express the same type of receptor, indicated by different colors of receptors and corresponding glomeruli in Figure 2. Projection neurons called mitral and tufted cells extend out of the OB and innervate several primary olfactory structures for subsequent processing of incoming olfactory information (Axel, 1995). The following primary olfactory regions will be discussed in depth: piriform cortex, olfactory tubercle, and cortical amygdala.

Piriform Cortex

Piriform cortex (Pir) is the largest and most understood primary olfactory structure (Giessel and Datta, 2014; Wilson and Sullivan, 2011). This structure is trilaminar and has subdivisions of each layer, unlike the neocortex, V1, or A1.

<INSERT FIGURE 3>

Layer Ia of Pir consists of mitral and tufted cell axons that send incoming information from the OB to different primary olfactory regions, while layer Ib consists of intracortical association fibers. There are small populations of inhibitory interneuron cell bodies throughout layer I, which allow for suppression of some incoming excitatory input (Wilson and Sullivan, 2011). Pyramidal cells extend through layer II, with apical dendrites extending into layer I and basal dendrites extending into layer III. Layer IIa, the most superficial portion of layer II, mostly receives input from mitral and tufted cells, and does not have much of an association role as Layer Ib does. Layer III consists of interneurons and somas of deep pyramidal cells (Wilson and Sullivan, 2011).

Pir receives direct input from the OB, and is therefore considered a primary olfactory structure (Wilson and Sullivan, 2011). A single OB glomerulus has mitral and tufted cells that extend across the lateral olfactory tract (LOT) along the ventral-lateral aspect of the brain and innervate Pir. These mitral and tufted projections disregard the spatial topography demonstrated in the OB and target Pir with dense and highly interspersed patterns of projections (Sosulski et al., 2011; Wesson and Wilson, 2011). The diffuse output from the OB and complex range of inputs into an individual piriform cortical cell allows for the classic divergence-convergence organization across the cortex

– a hallmark characteristic of Pir (Wilson and Sullivan, 2011). Individual Pir cells respond to multiple molecularly-diverse odorants (Rennaker et al., 2007). Cells that prefer a particular odor are spatially distributed across the cortex; therefore, neighboring cells demonstrate different response profiles and are uncharacteristic of the topographical organization demonstrated in the visual and auditory systems (Rennaker et al., 2007; Stettler and Axel, 2009).

Another feature of Pir is the presence of auto-associative intracortical fibers, which are Pir neurons that have few connections with Pir neurons in the same layer and close in proximity. This intrinsic network modulates incoming information by enhancing input through providing direct excitation to Pir neurons, or likewise suppressing input through activation of inhibitory interneurons (Wilson and Sullivan, 2011). This complex neural network suggests that this region is an associative cortex, meaning that this structure can identify the significance of a stimulus and plan and execute the appropriate response (Stettler and Axel, 2009).

Inhibitory interneurons also play a significant role in Pir activity. Pir can be classified as an auto-excitatory structure, which needs to be meticulously controlled to avoid over-excitation and ultimately seizure-like consequences. Inhibitory networks prevent this by modifying odor-evoked responses of individual Pir neurons (Wilson and Sullivan, 2011). Anatomical studies have confirmed projections of Pir output into the olfactory tubercle (Wesson and Wilson, 2011).

Olfactory Tubercle

The olfactory tubercle (OT), also a primary olfactory region with three layers, has two main divisions: a cortical zone and a cap or hilus zone, with various cell morphologies throughout each. Unlike Pir, the OT does not contain an association fiber system. OT receives various inputs of sensory information, such as from the OB, Pir, and anterior olfactory nucleus (Wesson and Wilson, 2011).

Pir and OT receive input from both mitral and tufted cells from the OB. However, mitral and tufted cells have different preferences for which primary olfactory region is targeted, shown in Figure 4.

<INSERT FIGURE 4>

Mitral cells tend to innervate Pir more so than OT, and tufted cells innervate OT more so than Pir (Figure 4). This suggests that Pir and the OT may serve alongside each other as parallel networks in olfactory processing. Tufted cells are more responsive to lower odor concentrations, are highly influenced by respiration cycles, and have broader receptive fields compared to mitral cells; these features may influence OT output to other regions (Mori and Shepherd, 1994; Shepherd, 2004).

The OT lies in the ventral striatum and plays a role in reward pathways considering its connectivity with several reward structures such as the nucleus accumbens, ventral tegmental area, and caudate putamen; this explains its involvement odor hedonics or preferences, and ultimately odor-motivated behaviors (Giessel and Datta, 2014; Wesson and Wilson, 2011). In a recent study, electrical stimulation of the

OT was found to be rewarding, and resulted in abolishment of odor preference and associated behaviors (Fitzgerald et al., 2014).

The OT is a site of multimodal sensory integration. Early olfactory processing in the OT is subject to modulation by auditory processing. Previous evidence of singular OT neurons responding to olfactory and auditory stimuli ultimately showed an additive effect in neuronal spike output (Wesson and Wilson, 2010).

OT neuron response properties have been previously described as characteristic of both the functional OB glomeruli units and the spatially distributed representation of information and lack of topography in Pir (Giessel and Datta, 2014). OT neurons were found to have broad responses to odor mixtures and also selective responses to monomolecular odorants, which may suggest that the OT plays a role in distinguishing odor identity (Giessel and Datta, 2014; Wesson and Wilson, 2010).

The OT receives input from the OB, Pir and amygdala (Giessel and Datta, 2014). The amygdala is also a primary olfactory region; the subdivisions of the amygdala that receive olfactory input have received relatively less attention than other areas involved in emotion and fear, and therefore should be further investigated.

Amygdala

The amygdala (AMG), a collection of numerous different nuclear and cortical divisions, is located in the temporal lobe. The AMG is better known for the significant role it plays in learning, memory, attention, emotion, and fear (Pitkanen et al., 1997). Its role in olfactory processing is often overlooked even though highly complex intra-amygdaloid connections allow for advanced processing of incoming sensory information.

The superficial amygdaloid nuclei, specifically the laminar cortical amygdala and the nuclear medial amygdala, are of interest to this study because they receive innervation from structures that process olfactory information (Pitkanen et al., 1997, Martinez-Marcos 2009; Winans and Scalia, 1970; Raisman, 1972; Scalia and Winans, 1975; Haplern, 1987; Xu et al., 2005; Licht and Meredith, 1987).

After sensory information enters the AMG, input goes through parallel processing across different divisions. Each division may have distinct functions and therefore process different components of information, resulting in a unique representation of the stimuli as a final output (Pitkanen et al., 1997). Overlapping projections within certain amygdaloid divisions allow for associative fine-tuning of information even during early stages of processing. Previous research showed that the flow of information within the AMG is reciprocal rather than unidirectional (Pitkanen et al., 1997). A reciprocal flow of information allows for a nucleus to self-regulate and to regulate other nuclei. This theory of reciprocal information flow is supported in rat subjects, but still has weak evidence in primate brains (Pitkanen et al., 1997).

There are three levels of connections within the AMG, or in other words, intra-amygdaloid connectivity. Internuclear connections exist between the 13 different amygdaloid nuclei. Each nucleus is further broken down into subdivisions; connections between these divisions are called interdivisional networks. Intradivisional connections exist within a single division (Pitkanen et al., 1997). These connections are depicted in Figure 5.

<INSERT FIGURE 5>

Previous research has established internuclear connections between the lateral, basal, and accessory basal amygdaloid nuclei (Pitkanen et al., 1997). Interdivisional connections have been established largely in lateral, basal, and central nucleus, and sparsely within accessory basal nucleus. Intradivisional connections have been established largely within basal, accessory basal, and central nucleus, and sparsely within lateral nucleus (Pitkanen et al., 1997).

The AMG is highly innervated by the OB which has two main divisions: the main olfactory bulb (MOB) and the accessory olfactory bulb (AOB). The MOB targets anterior cortical amygdala and posterolateral cortical amygdala – or in other words, olfactory amygdaloid nuclei, which detect various volatile odors. The AOB targets medial amygdala and posteromedial cortical amygdala, which are considered to be vomeronasal amygdaloid nuclei, which detect biologically relevant odors such as pheromones (Pro-Sistiaga et al., 2007, Martinez-Marcos 2009; Doty, 2003; Shipley, Ennis, and Puche, 2004). Anterior cortical amygdala and medial amygdala receive input from both the MOB and AOB (Pro-Sistiaga et al., 2007).

Additionally, Pir specifically innervates medial amygdala (MeA) and posterior cortical amygdala (plCoA) (Pro-Sistiaga et al., 2007). Because MeA had not been highly responsive in previous experiments, a recent study investigated odor response properties shared by Pir and plCoA through recording the activity of individual neurons in each region (Iurilli and Datta, 2017). Neurons in both Pir and plCoA demonstrated similar odor-tuning properties such as tuning breadth – or the range of odors cells respond to – in that there were no strong preferences for specific chemical odor classes in individual

neurons from either plCoA or Pir. A population of neurons in Pir and plCoA represent a distributive population code, where neuronal ensembles work together to represent sensory information across a cortex (Iurilli and Datta 2017).

Interestingly, only anterior and posterior cortical amygdaloid nuclei have previously shown to be odor-responsive on a population level (Pro-Sistiaga et al., 2007). Features of local circuitry within odor-responsive amygdaloid nuclei, and between these nuclei and other olfactory structures have been previously defined, but not well-characterized (Pitkanen et al., 2007). The local circuitry within the AMG warranted further investigation.

Current Study

This study investigated how odor representation is mapped across different primary olfactory structures. Preliminary research from the Cousens laboratory at Drew University was compiled and analyzed to understand the odor response properties of OT and AMG. Previous laboratory experiments used single tungsten electrodes and multi-site probes to record single unit activity in OT and AMG neurons in response to multiple sets of odorants. Previous literature about the odor response properties of Pir was used to make comparisons to our OT and AMG results.

Our overall research goal was to describe odor-response characteristics of OT and AMG neurons. We first characterized basic response properties including odor-responsivity, average basal firing rate, and odor selectivity to monomolecular odors which consisted of only one chemical, and pheromones which contained a mixture of chemicals.

Our first hypothesis was that OT neurons would demonstrate a broad tuning breadth; in other words, OT neurons would be highly responsive to preferred odors and relatively responsive to non-preferred odors. Previous research compared mitral and tufted innervation into Pir and OT. Tufted cells had a broader receptive field than mitral cells, or in other words, tended to respond to a larger set of odors than mitral cells did (Mori and Shepherd, 1994; Shepherd 2004). Pir received input predominantly from mitral cells and OT received input predominantly from tufted cells (Kang et al., 2010). We predicted that OT neurons would demonstrate similar features to the tufted cells it receives input from. If we previously collected data on Pir neurons, we would make similar assumptions according to source of input from the OB into Pir. Mitral and tufted cells innervate AMG to different extents depending on the amygdaloid nuclei (Kang et al., 2010). Because we did not have the complete set of histological data to analyze, we could not confirm which nucleus or division each of our isolated neurons were in. Therefore, we aimed to simply characterize tuning breadth of AMG.

Our second prediction was that OT and AMG neurons located adjacent to each other, or cell pairs, will likely demonstrate similar odor preferences, or correlated tuning. A 2011 article used a two-photon microscope to trace projections from a singular OB glomerulus to primary olfactory areas. In Pir, the OB glomerulus terminals were distributed and dispersed across the cortex. However, the data showed clumped glomerulus terminals in close proximity to each other – or patchy innervation – into the OT and AMG (Sosulski et al., 2011). From this, we hypothesize that adjacent neurons in

OT and in AMG will likely have similar odor preferences and will demonstrate correlated tuning.

Most isolated neurons in both OT and AMG were odor-responsive. There were more broadly-tuned individual neurons in AMG than OT. Overall, OT demonstrated a more narrow tuning breadth than AMG. Both regions were generally broadly-tuned. Only OT cell pairs demonstrated statistically significant correlated tuning, but upon visual analysis of histograms, there were twice as many OT cell pairs and one AMG cell pair that demonstrated correlated tuning. This may be explained by the nature of innervation from the OB, and by the methodology used to collect the data. Features of odor representation such as tuning breadth and correlated tuning have not been previously investigated in OT or AMG. Carriero (2009) examined connectivity between Pir and OT, and Iurilli (2017) compared odor features between Pir and AMG, but this current study made novel comparisons in odor features between OT and AMG.

Methods

The following surgical and electrophysiological procedures were conducted by Dr. Graham Cousens and previous students that worked in this laboratory (unpublished data). These experiments were conducted for various theses and research projects; I assisted with surgical and electrophysiological stages for some experiments. The current study compiled all previously collected data from this laboratory and analyzed it.

Rat Subjects

Sprague-Dawley rats weighing 270 to 480 grams (g) were housed in pairs. Cages were kept in a humidity and temperature-controlled vivarium and maintained on a 12-

hour light/dark cycle. Laboratory chow and water was available *ad libitum*. The following experiments met the US Public Health Service guidelines, and were approved by the Drew University Institutional Animal Care and Use Committee.

Surgical Procedures

Surgical procedures shown in Figure 6 were adapted from Stettler and Axel (2009).

<INSERT FIGURE 6>

A craniotomy was performed in the right parietal lobe, which allowed lateral-to-medial advancement of an electrode into the AMG. Cortex tissue around the middle cerebral artery was exposed, and an electrode was advanced medially through Pir. Rats were anesthetized with urethane (3.0 mg / kg, ip; isoflurane ip) and mounted in a stereotaxic frame. After exposure of the skull surface, an aluminum post was fixed to the posterior nasal bones with dental acrylic and skull screws. The subject was then repositioned for electrode advancement from above, with the left hemisphere facing up. Another small craniotomy in the left parietal lobe allowed placement of a reference electrode. The left masseter muscle was deflected, and the zygomatic bone and the anterior portion of the mandible were removed. Deflection of the temporalis muscle exposed the ventrolateral skull surface. A square window was created to expose the cortex near the middle cerebral artery approximately 1.0 – 4.0 mm posterior to Bregma.

Electrophysiological Recordings

An electrode was advanced medially with stereotaxic guidance through Pir. Recordings commenced once large spike waveforms > 2.0 mm were identified. Single-

unit activity was amplified (10,000x), filtered (500 Hz – 3 kHz) and digitized (20 kHz;

PCIe-6351, National Instruments, Austin, TX) for later offline analysis using Spike2

(Cambridge Electronic Design, Cambridge, UK). A thermocouple (Omega Engineering,

Inc., Stamford, CT) was placed slightly inside the nares of the subject to allow

monitoring of respiration phases. Waveforms were identified and isolated using

OfflineSorter (Plexon Inc., Dallas, TX). Individual cells were identified based on

waveform shape, waveform parameter clusters, and/or interspike interval histograms.

Other analyses were conducted using NeuroExplorer (Nex Technologies, Madison, AL)

or MatLab (The Mathworks, Natick, MA).

Stimulus Presentation

After a stable 2-minute baseline period was recorded, a sequence of 6 to 14

odorants was delivered in nitrogen at 1.0 L/min gas 2 - 4 centimeters (cm) away from the

nares of subjects using a custom-built flow-dilution olfactometer. There were two

categories of odors used: monomolecular odors and pheromones. Monomolecular odors

are "pure" in that these consist of only one chemical. Pheromones are odors released by

animals usually as a means of communication; pheromones contain a mixture of different

chemicals and may include monomolecular odors within them. The sequence of six

odorants consisted of the following: 1-heptanal (HNL), 2-heptanone (HNN), (R)-(+)-

limonene (LIM), isoamyl acetate (IAA), propyl butyrate (PBU), and 1,7-octadiene

(OCT). In addition to these six odorants, the following odorants were added to make

some combination of 14 odorants: 5-methyl-2-hexanone, cineole, cumene, ethyl acetate,

ethyl valerate, n-Nonane, fox urine, and cat urine. Combinations of these odors were

commonly used in a range of previous olfactory studies (Boyd et al., 2012; Fendt et al., 2005; Fitzgerald, Richardson, and Wesson, 2014; Gadizola et al., 2015; Iurilli and Datta, 2017; Poo and Isaacson, 2009 and 2011; Rennaker et al., 2007; Root et al., 2014; Stettler and Axel, 2009; Wesson and Wilson, 2010). All odorants were diluted to 350 parts per million in mineral oil. There was different timing in intervals between odor presentations depending on experiment as shown in Figure 7.

<center><INSERT FIGURE 7></center>

Odorants were presented for 2 seconds each, followed by either 30 seconds or 60 seconds between odor presentations, depending on number of odorants used, shown in Figure 7. Experiments that used six odors had 60 seconds between odor presentations, while experiments that used 12 or 14 odors had 30 seconds between odor presentations (Figure 7).

Histological Confirmation

Following data collection, brains were extracted and fixed in a 30% sucrose and formalin mixture for 10-14 days. Brains were sectioned in 50 μm sections, stained with neutral red for visualization of electrode localization. Not all histological data could be retrieved for the following analyses.

Data Analysis

The number of odors in experiments varied across experiments, but the data for the six common monomolecular odors that were used across all experiments were pulled out from the entire data set and analyzed as its own data set. Pheromone data for cat urine and fox urine were also retrieved from the full data set and analyzed. Neuronal firing

rates for 5 seconds before odor presentation (pre-odor) and 5 seconds after odor onset (post-odor) were obtained for a total interval of 10 seconds. Analyses were only conducted on odor-responsive neurons.

For odor responsivity experiments, firing rates for each neuron during each 10 second odor trial were averaged for each odor. The average change in firing rate was calculated by subtracting the average pre-odor firing rate from the average post-odor firing rate for each odor. These values were calculated for each odor and divided by the standard deviation (SD) of pre-odor firing rates for each odor to obtain z-scores, which describe how many SDs a value is away from the mean of the pre-odor firing rate, or the baseline activity. A cell was deemed responsive to an odor with a z-score of at least 2. If SD could not be calculated due to neurons exhibiting 0 Hz as average pre-odor activity, histograms of the 10 second firing period were created to visually evaluate neurons for odor responsivity. Subjective evaluation criteria for odor-responsive neurons included a sufficient increase in firing after an odor was presented at time = 0.

To analyze tuning breadth, post-odor firing rates for each neuron were averaged for each odor. Averages were sorted from greatest to least, or ranked from most- to least-preferred odor. Averages were converted to proportions. The most-preferred odor, or the odor with the greatest average, received a proportion of 1 and a rank of 1. Other averages were divided by this post-odor average to calculate proportions. The least-preferred odor received a rank of 6, due to 6 monomolecular odors being presented. Proportions across all neurons in one brain region were averaged for each rank. Standard error was calculated using proportions, and error bars were created using standard error of the

mean. An independent samples t-test was conducted on SPSS for each rank to test for differences in proportion of firing for each rank across brain regions.

To create interquartile range graphs (IQR) for monomolecular odor and pheromone data comparisons, z-scores were calculated as they previously were for odor-responsivity analyses. Z-scores were sorted from least to greatest. Quartiles were calculated: Q1 (25th percentile), Q2 (median), and Q3 (75th percentile). IQR graphs were created on Microsoft Excel using these values and the minimum and maximum z-score for each odor. For monomolecular odor analyses, a two-way repeated measures ANOVA was conducted on SPSS to examine main effects and interactions between odors and brain region. Pairwise comparison tests were run with SPSS to look for significant differences between odors. For pheromone analyses, a one-way ANOVA was conducted using SPSS to look for significant differences between how OT responded to both pheromones and an average of all z-score responses to monomolecular odors.

For correlated tuning calculations, z-scores for each odor were calculated and sorted from greatest to least. Z-scores were ranked from greatest to least, and received ranks of 1-6. For each cell pair, or two cells recorded on the same probe or with the same electrode within a recording session, pairwise comparisons tests were run in SPSS using Spearman's rho. Significant correlations were further investigated for cell-sorting errors using Offline Sorter to confirm that comparisons were not being made across the same neuron.

Results

Across 33 recording sessions in 16 subjects, 50 OT neurons and 50 AMG neurons were isolated. Only odor-responsive neurons were used for analyses. 35 OT neurons and 33 AMG neurons were deemed odor-responsive and analyzed to describe characteristics of odor-responsivity in OT and AMG neurons. Our study investigated general responsivity, tuning breadth, and correlated tuning in adjacent cell pairs.

Basic Odor-Response Properties

Only odor-responsive neurons were used to describe odor response characteristics of OT and AMG; an example of an odor-responsive neuron is shown in Figure 8.

<INSERT FIGURE 8>

Figure 8 showed the responses of one tubercle neuron – cell C, recorded on Site 5 of the probe – to six monomolecular odors. Neurons were characterized as odor-responsive if the average firing rate during the post-odor period was at least ± 2 SD away from the average firing rate during the pre-odor period. Cell C was characterized as odor-responsive because the change in firing rate after odor presentation was at least ± 2 SD for five of the odors presented (Figure 8). However, some neurons had a low firing average or did not fire during the pre-odor period, so the SD could not be calculated. These neurons were categorized as odor-responsive by subjective evaluation of histograms that depicted neuronal firing during the five-second period before and after an odor was presented. Figure 8 was an example of a histogram analysis. Neurons with low pre-odor firing were considered odor-responsive by subjective evaluation if there was an increase in frequency during the post-odor period at least twice in magnitude of the pre-

odor firing. For example, if Cell C were to be categorized as odor-responsive by subjective evaluation, Cell C would be considered responsive to OCT, PBU, HNN, and IAA, but not responsive to HNL or LIM (Figure 8). Neurons with no pre-odor firing (or an average of 0Hz) were considered odor-responsive if there was a noticeable spike in firing during the post-odor period. 17% of isolated neurons exhibited an average of 0Hz of firing during the pre-odor period, and were subjectively evaluated (data not shown); 9/18 of those neurons were characterized as odor-responsive, according to our subjective histogram analysis.

Neurons were also characterized by tuning properties. Neurons were characterized as broadly tuned if responsive to more than one odor presented, and narrowly tuned when responsive to only one odor presented. For instance, as seen in the histogram Cell C was responsive to OCT, PBU, HNN, and IAA, and therefore characterized as broadly tuned (Figure 8). The odor-response characteristics of the neurons isolated in OT and AMG are summarized in Table 1.

<INSERT TABLE 1>

As shown in Table 1, the majority of OT and AMG neurons were characterized as odor-responsive; the firing rate and magnitude of response in approximately 2/3rds of neurons isolated in both regions were affected by the presence of odor stimuli. This was expected considering the OT and AMG are both primary olfactory structures and receive direct input from the OB. Average basal firing rates during the pre-odor period were not statistically different between OT and AMG. 2 – 6 Hz was a typical magnitude of firing during the five-second pre-odor period for both OT and AMG neurons (Table 1). This

was expected because neurons communicate and are involved in local networks, and exhibit minimal firing without stimulation. Among the AMG neurons, there was a basal firing rate outlier of 68.15 Hz from one neuron (data not shown); if removed, the average basal firing rate for AMG would be 2.96 Hz $\pm$ 0.70. As shown in Table 1, there were a larger proportion of broadly tuned individual AMG neurons than individual OT neurons. However, the majority of isolated OT neurons were still broadly tuned, which supports our hypothesis that OT neurons would generally demonstrate broad tuning.

Neurons elicit different responses depending on the stimulus. Overall neural activity of a region varied across odor identities, as in Figure 9 shown with interquartile ranges.

<INSERT FIGURE 9>

Both the OT and AMG showed overall excitatory responses to each of the six monomolecular odors presented. According to the results of the two-way repeated measures ANOVA, there was a main effect of odor, F (4.91, 93.34) = 5.039, $p < 0.0005$. Pairwise comparisons were conducted for each odor. Data were presented using z-scores and interquartile ranges. OT and AMG neurons respond similarly to each odor, but different odors elicit different magnitudes of response from neurons in both regions (Figure 9). For example, OT and AMG respond with similar magnitudes in comparison to each other in response to OCT. This similarity is maintained across most odors; OT and AMG respond with similar magnitudes in response to LIM as well (Figure 9). However, there was a main effect of odor, or in other words, different odors elicited different magnitudes of responses from both regions. As shown in Figure 9, neurons in the OT

overall seem to be the most excited by OCT, and least excited by HNL and LIM, which

does have a statistically significant difference ($p < 0.0005$). Multiple features of these

monomolecular odorants may explain these results, such as molecular weight or

functional group. We investigated molecular weight, and found that all six odors range

between $110 - 137$ g/mol; thus, this range was not wide enough to associate molecular

weight with a brain region's overall response to an odor. The chemical composition of

each odorant may play a role in neuronal activity. Neurons may be selective to specific

orientations of an odor chemical structure or a certain functional group that several

odorants share.

Our study investigated responsivity of these regions to monomolecular odorants;

OT neurons were also presented with two pheromones, which are biologically relevant

and consist of a mixture of chemicals. Pheromone data was not collected for AMG

neurons. Although no statistical significance was found, Figure 10 showed the

comparison between both pheromones and an overall response to monomolecular odors.

<INSERT FIGURE 10>

OT neurons showed overall excitatory responses to monomolecular odors as a

whole and cat urine and fox urine, as seen in Figure 10. According to the one-way

ANOVA conducted, there were no statistically significant differences detected. The OT

showed similar responses to both pheromones and an average of all six monomolecular

odors used (Figure 10). There were significantly more neurons receiving the six

monomolecular odorants; the small sample size of neurons ($N = 29$) receiving the

pheromones may have resulted in biased data. If the sample was larger for experiments

using pheromones, we would expect a larger excitatory response. There were more components in the pheromones, which may result in a greater possibility of neuronal excitation. Considering there was a mixture of chemicals within the pheromones, it is unknown as to which component of the cat and fox urine resulted in excitation of OT neurons. Pheromone data were not collected while recording in AMG, which would be an interesting future direction considering the AMG is the brain region well-known for processing fear. We would expect heightened AMG responsivity, especially in response to fox urine and cat urine, which are natural predators of rats.

Odor Tuning Breadth

Tuning breadth contributed to characterizing odor response properties of OT and AMG, and provided insight to how selective these regions were to responding to different odors. Although individual neurons each have unique tuning breadths, our hypothesis addresses the tuning breadth of the OT and AMG on a wider scale, or how each brain structure as a whole responds and how each can be categorized in tuning breadth. Figure 11 compared tuning breadths of OT and AMG according to odor rank calculations.

<INSERT FIGURE 11>

It was expected at earlier ranks that there would be no difference in magnitude of response; if neurons preferred an odor, they elicited a greater response. However, there was a difference between OT and AMG neurons in magnitude of responsivity to the least-preferred odor (Figure 11). According to the independent samples t-test conducted, there was a trend at Rank 6, $t_{61} = 1.830$, $p = 0.072$. In response to the least-preferred monomolecular odor, OT neurons demonstrated a narrower tuning breadth than AMG,

indicated by a steeper slope shown in Figure 11. OT neurons were more selective with

which odors they responded to, and had less intense responses to their least-preferred

odor; the lower proportion of firing caused a steeper slope (Figure 11). On the other hand,

although AMG neurons preferred Rank 6 odors the least, those neurons fired with greater

magnitude than OT neurons. This created a flatter slope in Figure 11, suggesting broader

tuning in AMG neurons relative to OT neurons. Although the OT had a more narrow

tuning breadth than AMG, both regions support our hypothesis that OT would generally

demonstrate broad tuning because both regions could generally be described as

demonstrating broad tuning.

Correlated Tuning in Adjacent Cell Pairs

Among 33 recording sessions, there were 51 OT cell pair comparisons and 15

AMG cell pair comparisons. Neurons were paired for analysis if they were recorded on

the same multi-site probe or recorded with single electrodes during the same session. An

example of correlated tuning among a cell pair seen by subjective evaluation is shown in

Figure 12.

<INSERT FIGURE 12>

The responses of two AMG neurons – cell A and cell D, recorded simultaneously

on a probe – in response to the same six monomolecular odors is shown in Figure 12.

Cell pairs were characterized to demonstrate correlated tuning if both cells were odor-

responsive to at least one common odor presented. As seen in Figure 12, both cells A and

D were clearly odor-responsive to HNL, OCT, and PBU. The remaining odors may have

elicited slight responses in these cells, but the change in firing rate compared to the five-

second pre-odor period was not convincing enough to be odor-responsive (Figure 12). This cell pair was categorized as odor-responsive because both were odor-responsive to more than one common odor, and in fact, multiple common odors (Figure 12).

Cell pairs were also characterized to demonstrate correlated tuning by statistical analysis and by visual analysis of histograms of adjacent cell pairs. Table 2 summarizes the different measures used to determine correlated tuning in cell pairs in the OT and AMG.

<INSERT TABLE 2>

The majority of OT cell pairs were recorded with multi-site probes, while AMG cell pairs were recorded during the same recording session using a single electrode at different depths (Table 2). Correlated tuning among cell pairs was calculated using Spearman's rho to analyze comparable ranks in odor preference. According to the pairwise comparisons test that was conducted using odor ranks, there was a trend that supported that four cell pairs in OT were correlated, shown in Table 2. There were no statistically significant correlated cell pairs in AMG (Table 2). However, upon subjective evaluation of cell pairs, there were eight OT cell pairs and one AMG cell pair that demonstrated correlated tuning. Some extent of correlated tuning was demonstrated in both brain regions; OT demonstrated stronger correlated tuning in that correlations were detected by statistical analyses, while there was only one example of correlated tuning in AMG. When less strict thresholds were set for correlated tuning, such as through visual evaluation of histograms for increases in firing rate during odor presentation, more correlated cell pairs were identified. Our hypothesis that both regions would demonstrate

correlated tuning was better supported by the results from the visual analysis of histograms, compared to the results from the statistical analyses. These findings may be explained by the different methods used to collect data from each region. OT neurons were predominantly recorded on multi-site probes, where increments between recording sites were known. AMG neurons were recorded using single tungsten electrodes. AMG cell pairs consisted of either the spikes of two neurons being simultaneously recorded or spikes recorded at different locations during the same recording session. Additionally, cell pairs could have consisted of cells recorded on the edge of patches; if one patch of neurons had slightly different odor preferences than the adjacent patch of neurons, adjacent neurons may have been close enough in proximity to be recorded on the same probe or single electrode but may have had similar odor preferences that were different enough to be quantified as a weak correlation in statistical analyses.

Discussion

The major objectives of this study were to characterize features of odor processing in OT and AMG neurons. Features of odor processing include odor responsivity, tuning breadth and correlated tuning of adjacent cells. This study compiled and analyzed preliminary data collected by previous Cousens laboratory students and Dr. Cousens, which consisted of electrophysiological recordings of how individual neurons in OT and AMG responded to a set of odorants.

Basic Odor-Response Properties

Odor Responsivity

The majority of neurons recorded in OT and AMG were odor-responsive, with proportions shown in Table 1. This result was expected because the OT and AMG are both primary olfactory regions. This confirms that both structures process olfactory information. Only odor-responsive neurons were used for these analyses, with an example odor-responsive neuron shown in Figure 8.

A previous study by Wesson and Wilson (2010) characterized OT neurons as odor-responsive both on a population level and an individual cellular level. This study found 64% of tubercle neurons to respond to at least one presented odorant out of the five monomolecular odorants used in their experiments (Wesson and Wilson, 2010). The set of experiments analyzed in our study presented at least six odorants, including pheromones in the larger odor sets. Considering this, our experiments may have resulted in a greater proportion of odor-responsive OT neurons (70%, Table 1) due to a larger odor set and a greater variation of presented odors, or biological variability among neurons.

Basal Firing Rate

We analyzed 5 seconds before and 5 seconds after the onset of odor presentations because the onset of response to odors began after the 2 second odor presentation for some neurons. Responses to odors also lasted longer than the 2 second odor presentation for some neurons. Average basal firing rates during the 5 second pre-odor period were typically 2 – 6 Hz for both OT and AMG neurons, shown in Table 1. This was expected

because neurons communicate and are involved in local networks, and exhibit minimal firing without stimulation. If the outlier basal firing rate was removed from the AMG data set, both OT and AMG would have average basal firing rates of approximately 3 Hz.

A 2010 study examined odor response in OT neurons and calculated the average basal firing rate using firing from 2 seconds before odor stimulation; a majority of basal firing rates were less than 5 Hz (Wesson and Wilson, 2010). This experiment additionally evaluated OT neuron activity in response to auditory stimuli to assess the role of tubercle in processing multiple types of sensory information. The activation of different sensory pathways may have influenced their results for neuronal firing in tubercle (Wesson and Wilson, 2010). Another study conducted recorded tubercle responses in awake mice to understand the role of tubercle in odor valence, or in other words, distinguishing between components of an odor. The basal firing rate was calculated using 2 seconds before the odor was presented. The average basal firing rate was 1.9 spikes/second and had a range of 0 - 77.8 Hz (Gadizola et al., 2015). Both studies experienced few high basal firing rates as well (Wesson and Wilson, 2010; Gadizola et al., 2015). These drastic fluctuations in basal firing rates may be explained by the set of conditions depending on the experiment. If a neuron detects a highly-preferred odor or has a longer onset in its response to an odor presentation, residual neuronal firing may have overlapped with the proceeding 5 second pre-odor period and lead to a higher average basal firing rate. Neither study conducted AMG neuron recordings.

Odor Selectivity

OT and AMG neurons responded with similar magnitudes to each monomolecular odor presented, yet the presentation of different odors elicited different responses in OT and AMG neurons, shown in Figure 9. For example, OT neurons and AMG neurons both showed similar magnitudes of excitation in response to IAA. OT neurons and AMG neurons both showed similar magnitudes of excitation also in response to OCT. However, the magnitude of excitation in response to IAA is less than the magnitude of excitation in response to OCT. Therefore, OT and AMG have similar response properties to the same set of odors, and respond differently to various odors. This may be explained by connectivity within each region as well as sources of input into each region, and contributes to understanding more about the various types of odors that can elicit responses in the OT and AMG structures overall.

The OT and AMG receive input from additional olfactory regions besides the OB; OT is innervated by Pir and predominantly tufted cells from the OB, while the AMG is heavily innervated by Pir and both divisions of the OB (Wesson and Wilson, 2011; Pro-Sistiaga et al., 2007). These additional olfactory regions may influence the output of OT and AMG neurons, or more specifically, may enhance excitation or inhibition. Although there were no noticeable inhibitory responses in our results, excitatory responses may have been affected.

The OT also shares connections with the reward pathways of the brain, and even has the ability to activate structures involved with motivationally-guided behaviors. If a highly-preferred odor is presented, the reward system may be activated because of the

motivation to further process the odor, which may lead to recruitment of additional OT

neurons (Fitzgerald et al., 2014). Further research on the appetitive and aversive nature of

these six monomolecular odorants would provide more insight to the odor selectivity of

OT neurons. Furthermore, the OT is a multi-modal processing unit and also responds to

auditory stimuli (Wesson and Wilson, 2011). Brain recordings were not conducted in a

sound-free environment; the noise from equipment used to record and display brain

activity may have biased OT neuron recordings. Multiple pathways of incoming sensory

input may have resulted in an additive effect and ultimately increase the responsivity of

OT cells to odor stimuli. This strong connectivity with different sensory regions may

explain the nature of OT neuron responses to odor presentation. There are three levels of

connections within the AMG, or in other words, intra-amygdaloid connectivity:

internuclear connections, interdivisional networks, and intradivisional connections,

depicted in Figure 5. These networks may play a role in the responses of AMG neurons.

Because complete histological data was not available, some recordings may have been in

MeA, which seems to be unresponsive to odor stimulation in previous studies; this could

have washed out the more excitatory responses of AMG neurons.

A previous study by Root (2014) found that cortical amygdala (CoA) neurons

showed excitatory and inhibitory responses to a set of 17 odors. Neurons showed the

most excitatory responses to appetitive odors such as peanut oil, and the most inhibitory

responses to aversive odors such as TMT (Root et al., 2014). A more recent study

examined a subdivision of CoA, the posterolateral CoA (plCoA); they found that plCoA

neurons were responsive to the three odors presented, all of which resulted in slight

differences in behavior in awake rat subjects (Iurilli and Datta, 2017). CoA is the first target of olfactory input into the AMG (Mouly, 2004). Further research into the appetitive or aversive nature of these six monomolecular odors may provide insight to the common selectivity to certain odors in OT and AMG neurons.

OT Responsivity to Pheromones

OT neurons responded to pheromones in a similar way to the responses to monomolecular odors overall, shown in Figure 10. This was a novel observation because there are no previous studies that investigate the effect of pheromones on OT responsivity. These results contribute to understanding the different categories of odors and types of sensory stimuli that OT is responsive to. In future studies, it would be interesting to see whether OT neurons can break down the components of the mixture and can specifically respond to the monomolecular properties. To examine this, future studies could isolate TMT from fox urine and observe the effects on individual neuron responses and how the brain region responds as a whole. Additionally, there was no pheromone data collected on AMG cells. Previous research regarding fearful behavioral responses are available, but applying these methods would contribute to the responses properties of individual AMG neurons due to induction of fear with predator odors.

<u>Odor Tuning Breadth</u>

In order to test the hypothesis that OT neurons would demonstrate a broad tuning breadth and describe the tuning breadth of AMG neurons, average changes in firing rate were converted into proportions and given ranks. All most-preferred odors were compared to subsequent ranks until the least-preferred odors were reached, shown in

Figure 11. Neurons recorded in both OT and AMG demonstrated broad tuning breaths in response to monomolecular odors, supporting our hypothesis. In response to the least-preferred odors, OT neurons were more selective to which odors they were and were not responsive to, and responded less than AMG neurons (Figure 11). This finding is consistent with the innervation to OT by predominantly tufted cells, as in Wesson and Wilson's previous study (2011). Establishing broad tuning in these regions contributes to a further understanding of how the neurons that make up these structures function and overall, how these regions process sensory information. Further analyses with electrode localization and AMG connectivity with other brain structures would have to be conducted to understand why AMG neurons have an even broader tuning breadth than OT.

A study with similar analyses found that neurons in anterior Pir demonstrated a broader tuning breadth than neurons recorded in lateral entorhinal cortex (Xu and Wilson, 2012). Pir data was not previously collected in the Cousens laboratory, so this 2012 study allowed for comparisons between previous Pir research, and current OT and AMG data collected in this lab. In comparison to our OT and AMG tuning breadth slopes shown in Figure 11, Pir and lateral entorhinal cortex slopes from this previous study seem to be steeper, demonstrating a relatively narrower tuning to odors (Xu and Wilson, 2012). This may be explained by the innervation of mitral and tufted cells from the OB into these regions. Tufted cells demonstrated a broad tuning breadth while mitral cells demonstrated a relatively more narrow tuning breadth, according to Wesson's and Wilson's study (2010). Although OT and Pir receive innervation from both tufted and mitral cells from

the OB, OT receives input predominantly from tufted cells while Pir receives input predominantly from mitral cells (Wesson and Wilson, 2010). Therefore, it is likely that neuronal activity from a cell mimics the activity features of the structures that neuron receives input from.

Innervation into a structure by just a few mitral or tufted cells has elicited neuronal responses; these projection neurons from the OB hold a very powerful influence (Franks and Isaacson, 2006). However, a previous study found that this influence was washed out in Pir by the presence of intracortical association fibers. Even though the mitral and tufted cells relay excitatory input into Pir, the inhibitory layer of interneurons process the information as well, ultimately silencing some of the excitatory input (Poo and Isaacson, 2011). The lack of these inhibitory interneurons in OT may explain why OT neurons demonstrate a broad tuning breadth relative to Pir neurons.

Correlated Tuning in Adjacent Cell Pairs

In order to test the hypothesis that both OT and AMG would demonstrate correlated tuning, adjacent neurons were coupled into cell pairs and analyzed through statistical analyses and visual inspection of histograms to further understand the extent of correlated tuning in each brain structure. An example of correlated cells is depicted by Figure 12. Both neurons are responsive and unresponsive to the same odors (Figure 12). A summary of statistical results and subjective evaluation of correlated tuning in adjacent neurons within both regions are listed in Table 2. Our hypothesis that both regions would demonstrate correlated tuning was not supported; there were few correlated OT cell pairs that were only supported by a statistical trend, while no significant cell pairs were

correlated in AMG. Upon visual inspection of cell pair histograms, there were twice as many OT cell pairs considered to be correlated and one AMG cell pair (Table 2). However, this is not strong enough to fully support our hypothesis; only OT demonstrated correlated tuning, while AMG did not. Data files for correlated cell pairs were further investigated in Offline Sorter to confirm that cell sorting – or differentiation of one neuron from another – was sufficient. In other words, these files were double-checked to ensure that one neuron was not accidentally classified as two neurons that have similar odor preferences. While OT may be organized in smaller segregated patches, AMG may be organized more like Pir and demonstrate spatial distribution.These findings provide insight to the local circuitry of each of these brain structures; local networks often govern fine-tuned modulations to incoming information, and play an important role in processing stimuli.

Coupled with Pir findings by Stettler and Axel (2009), our findings support Sosulski's paper that AMG neurons are organized similar to Pir (2011). Pir was previously found to demonstrate discontinuous receptive fields, where similar stimulus features did not vary smoothly and gradually across cortical space, as it typically does in other sensory systems (Stettler and Axel, 2009). Therefore, two adjacent Pir neurons rarely shared similar odor preferences. If an ensemble of neurons were seen to be odor-responsive after one odor presentation, one neuron in this ensemble likely responded to multiple dissimilar odorants. This may be due to convergence of different mitral and tufted cells on an individual Pir cell (Stettler and Axel, 2009).

Sosulski's study showed a patchy innervation of OB glomeruli into the OT and AMG (Sosulski et al., 2011). This finding was not heavily supported by our results because the majority of OT cell pairs were not correlated by statistical analysis and by visual inspection of neuronal activity on histograms. Our AMG findings were also unsupported in this paper as well; this is because there were no statistically significant correlated cell pairs and only one correlated cell pair through visual inspection, which is a qualitative analysis and is the weaker of the two measures of correlated tuning. The correlated cell pairs in OT and AMG that we did find may have consisted of neurons on the edge of a patch, which may explain why there was some extent of similar odor preferences but not strong enough to be supported by statistical analysis. This may also be explained by the concept that OT has smaller segregated patches of neurons clustered together that respond to similar odors, while AMG is more organized like Pir with spatially distributed neurons responding to odors.

Conclusions

This study made novel comparisons between and investigated the odor response properties of neurons in OT and AMG – two primary olfactory regions. Odor response properties on an individual cell level have not been previously well-defined for these regions. The majority of isolated neurons in both regions were odor-responsive, confirming that both are involved in olfactory processing. Further analyses should be conducted on the characteristics of each monomolecular odor and pheromone to better understand neuronal responses to those stimuli. Our first hypothesis was supported in that OT demonstrated a broad tuning breadth in response to monomolecular odors. This

suggests the OT receives sufficient input by tufted cells from the OB. The AMG

demonstrated a broader tuning breadth than OT, which may suggest that the nuclei we

recorded in also receive innervation from tufted cells. Further histological analyses could

confirm the exact nuclei that were penetrated. Our second hypothesis was supported by

OT neuron results but not by AMG neuron results. There were very few OT cell pairs

that demonstrated significant correlated tuning, which suggests that the segregated

clusters of neurons that respond to similar sensory information may be smaller than

expected. No AMG cell pairs demonstrated correlated tuning, which suggests that AMG

may be more organized like Pir, which has a spatially distributed set of neurons that is

different in response to each odor presented. This study further contributes to

understanding how individual neurons in both regions respond to odor stimuli, as well as

how each region functions as a whole in response to olfactory input.

Figures and Tables

Figure 1: Sensory Stimuli Organized across Layers or Columns across Different Sensory Systems. A. Neocortex organized by columns and layers. B. Primary visual cortex is organized by orientation columns. C. Primary auditory cortex is organized by frequency columns.
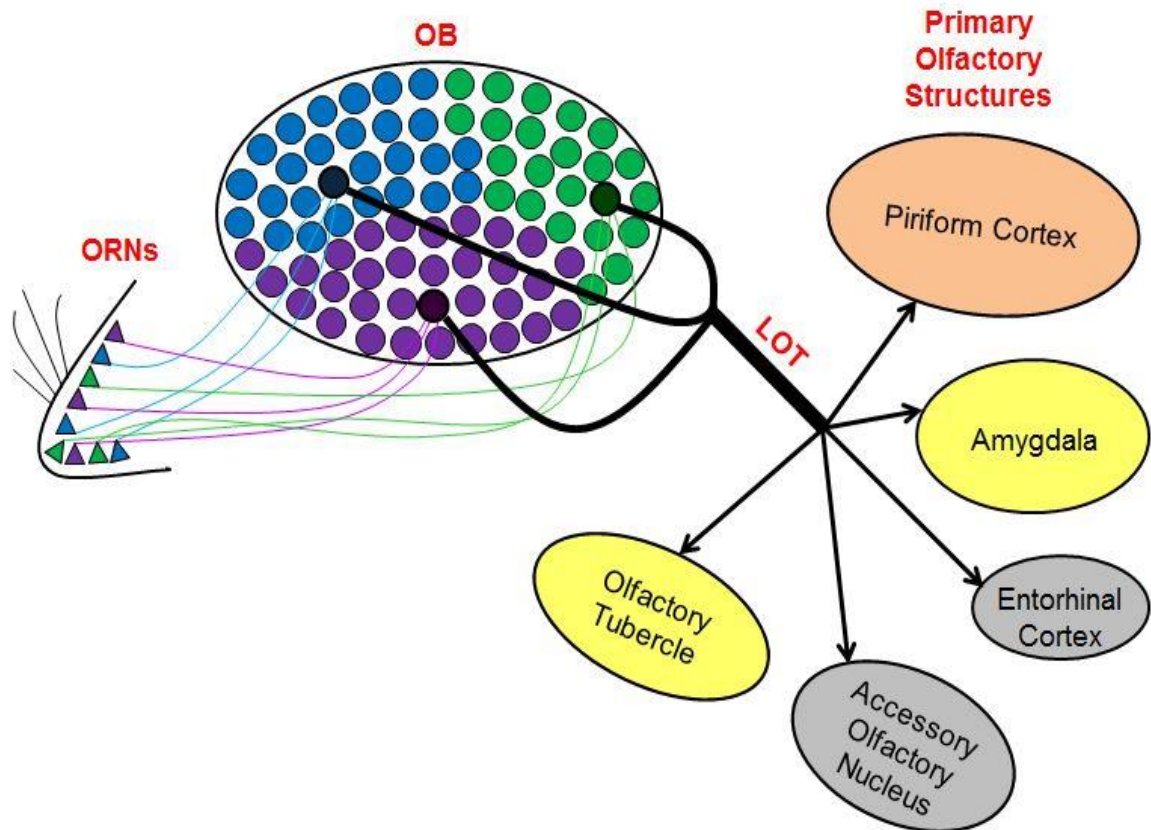
Figure 2: Odor Processing Pathway in the Olfactory System. Odors are detected by ORNs. Information sent to OB, organized in glomeruli, and sent through LOT to project to various primary olfactory structures.
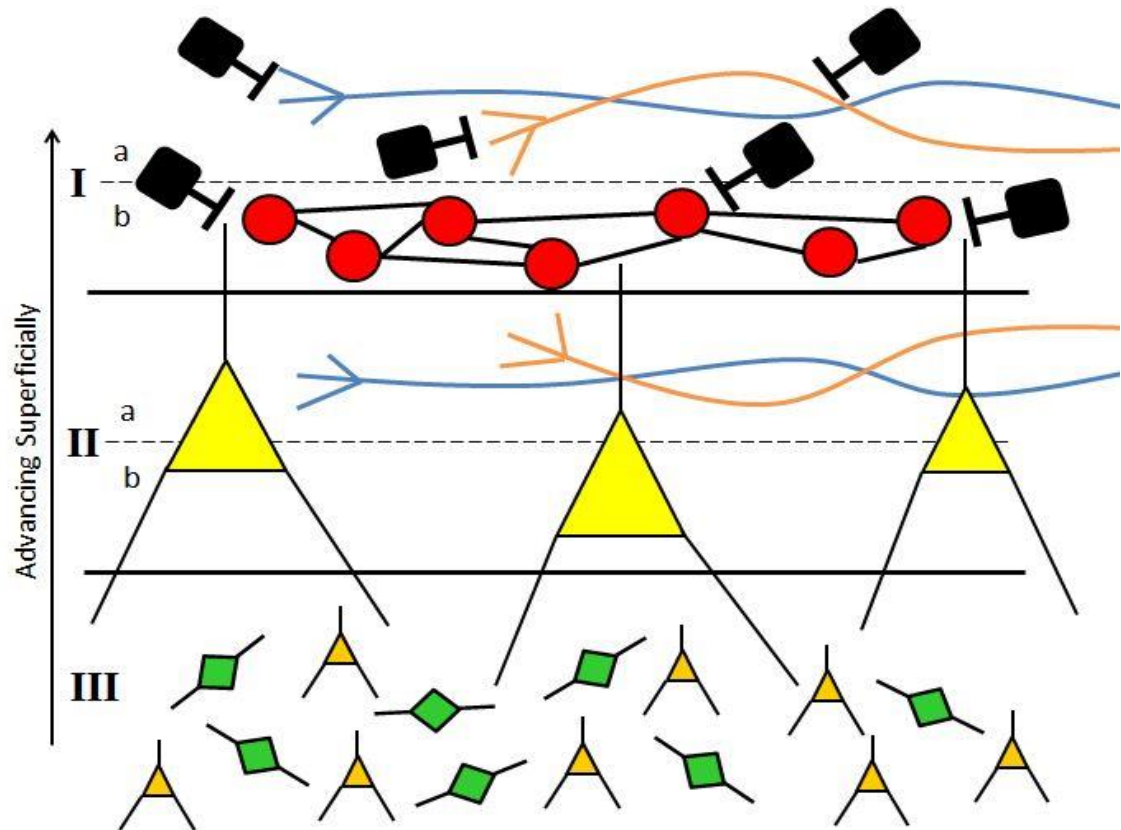
Figure 3: Sensory Information Organized across Layers in Pir. Blue and orange projections indicate mitral and tufted cells. Black square cells indicate inhibitory interneurons. Red circular cells indicate intracortical association fibers. Yellow triangle cells indicate pyramidal cells. Green diamond cells indicate
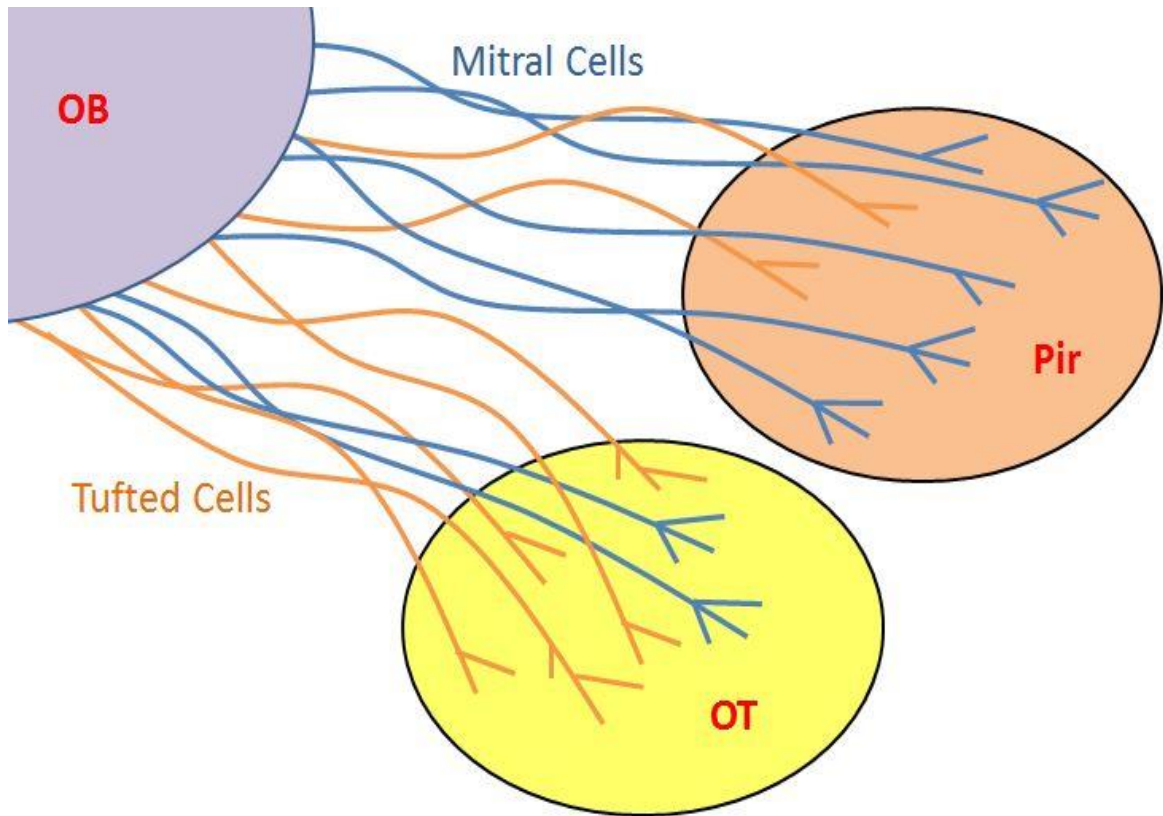
Figure 4: Mitral and Tufted Cell Innervation to Primary Olfactory Structures.
Mitral cells indicated by blue projections from OB. Tufted cells indicated by orange projections from OB.
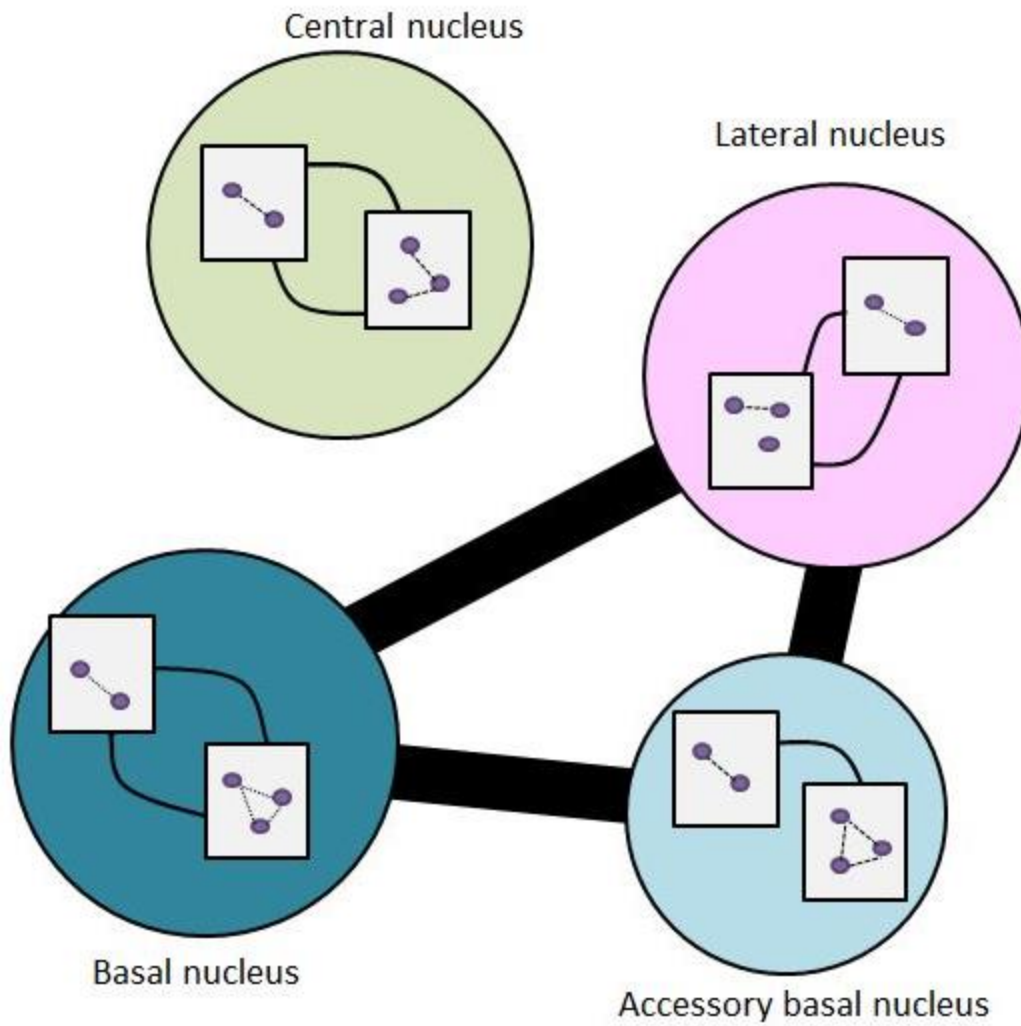
Figure 5: Amygdaloid Nuclei Organization: Internuclear, Interdivisional, and Intradivisional Connections. Thickest solid lines indicate internuclear connections. Thin solid lines indicate interdivisional connections. Dashed lines indicate intradivisional connections.
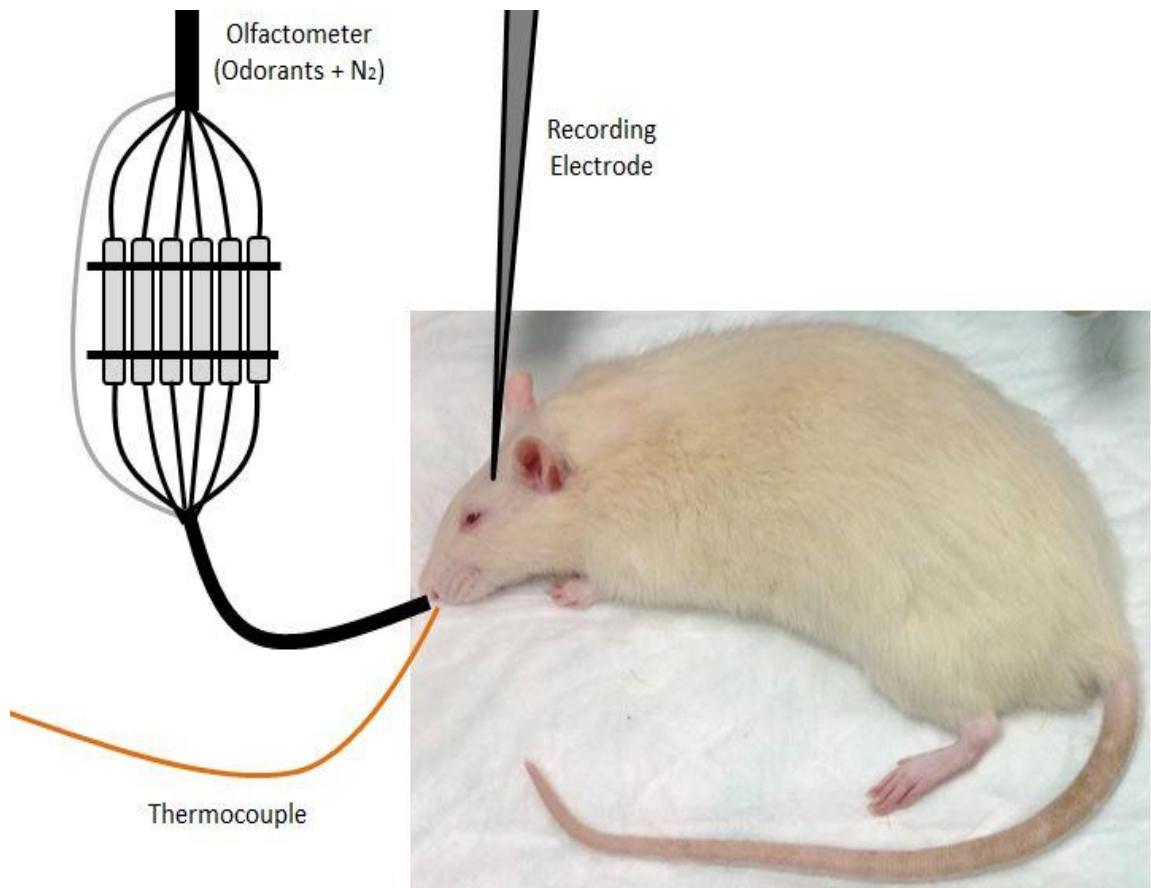
Figure 6: Surgical Procedures. Odorants presented to subject nares through olfactometer. Thermocouple monitors respiration cycles. Recording electrode placed into brain region of interest.

2 seconds odor   30 or 60 seconds N$_2$ gas   2 seconds odor   30 or 60 seconds N$_2$ gas
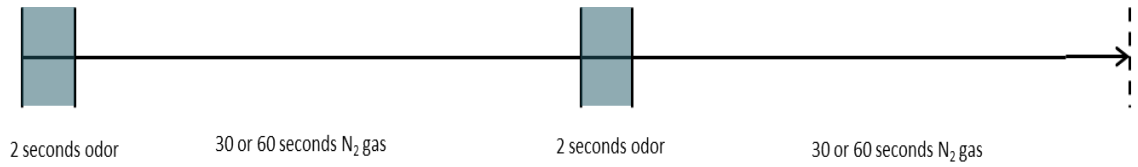
Figure 7: Odor Presentation Schedule. Different interstimulus intervals depending on experimental conditions. Experiments using six odors had an interstimulus interval of 60 seconds. Experiments using 12 or 14 odors had an interstimulus interval of 30 seconds.
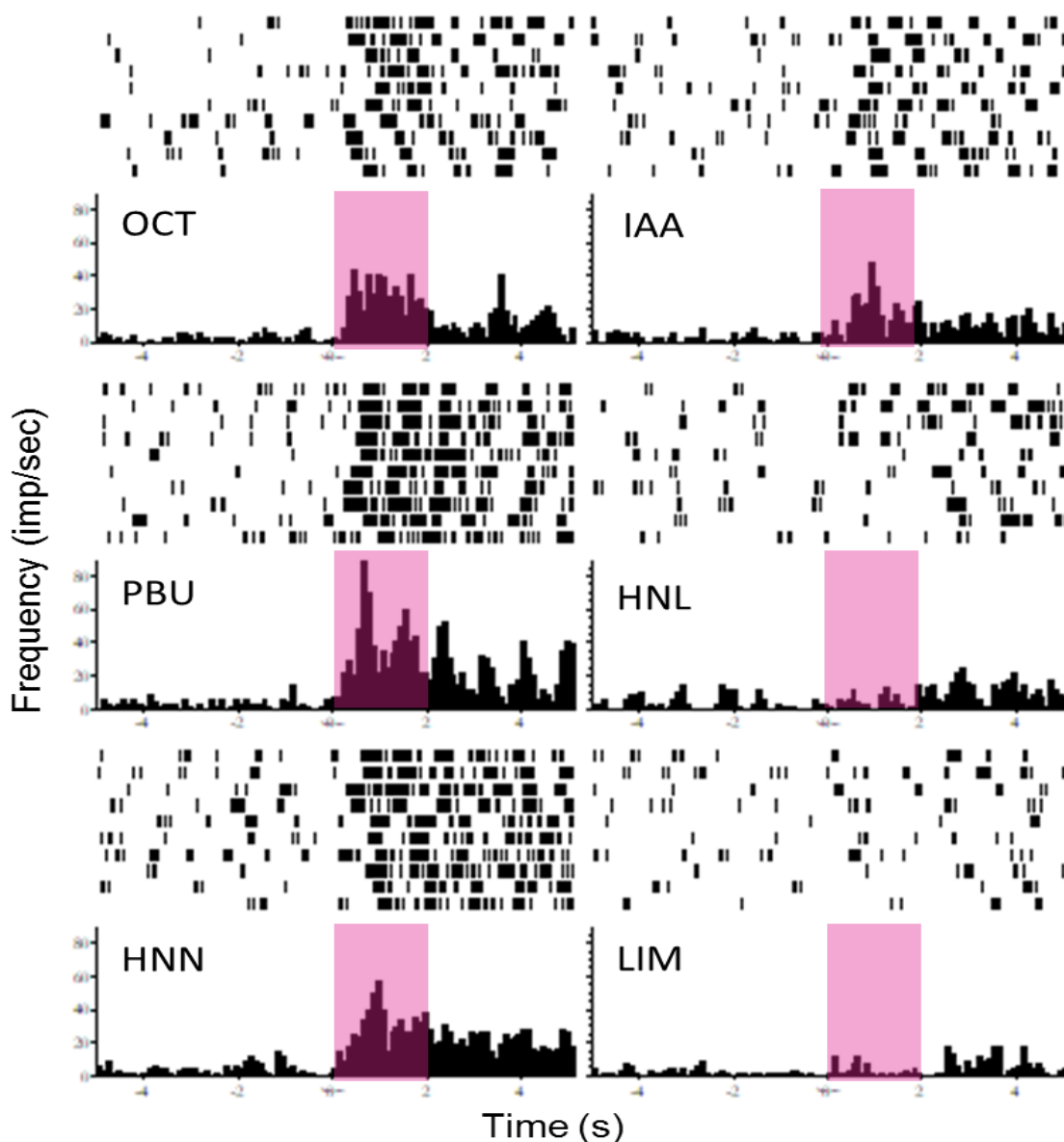
Figure 8: Neurons Characterized according to Odor Responsivity. Isolated tubercle cell, cell C, exposed to six monomolecular odors (File A10_2475). Number of rows in raster plots above indicate number of odor trials. Neuronal spikes are indicated by black vertical dashes. Histograms below average spike activity in the corresponding raster plot. Cell C was characterized as odor-responsive by subjective evaluation; post-odor firing reaches twice the frequency as pre-odor baseline firing for more than one odor. Cell C was characterized as broadly tuned by subjective evaluation; sufficient change in firing in response to more than one odor. Odor presentation (2 seconds) indicated by pink highlighted region.

Table 1: Characterizing Isolated Neurons in OT and AMG

	OT	AMG
Total Neurons Isolated	50	50
Odor-Responsive Neurons	35 / 50 70%	33/50 66%
Average Basal Firing Rate	2.98 ± 0.82	4.32 ± 1.54
Broadly-Tuned Neurons	23 / 35 65.7%	29 / 33 87.9%
Narrowly-Tuned Neurons	12 / 35 34.3%	4 / 33 12.1%

*Data obtained by SEM.
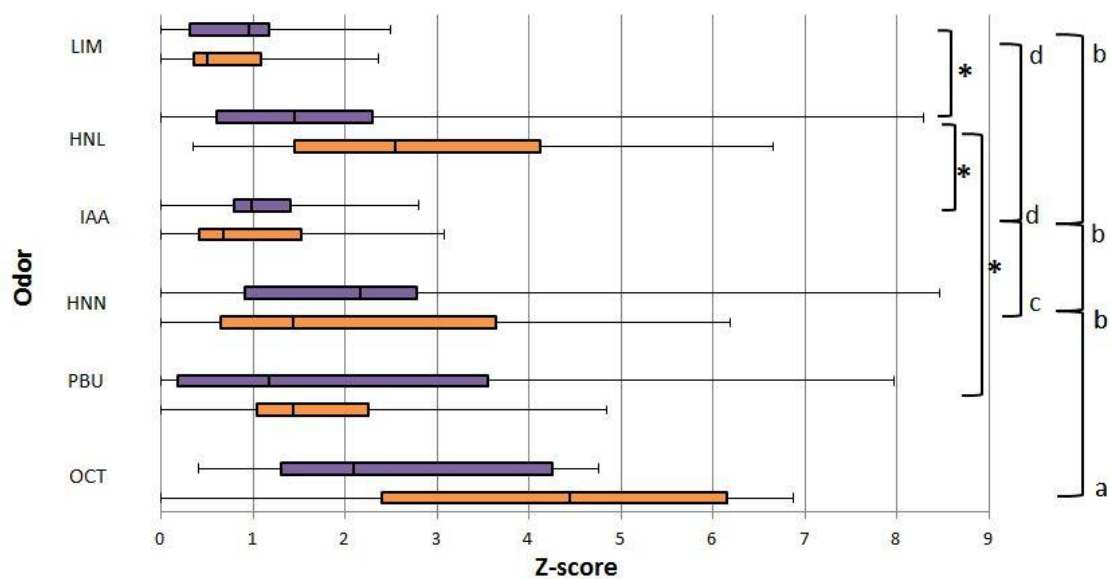
Figure 9: Responsivity of Region according to Odor Identity. AMG indicated in purple. OT indicated in orange. Main effect of odor. Data obtained by z-scores and interquartile ranges. Minimum represented by first "error bar"; maximum represented by last "error bar." (A) different from (B's), (C) different from (D's). *$p < 0.05$, [a-c]$p < 0.05$.
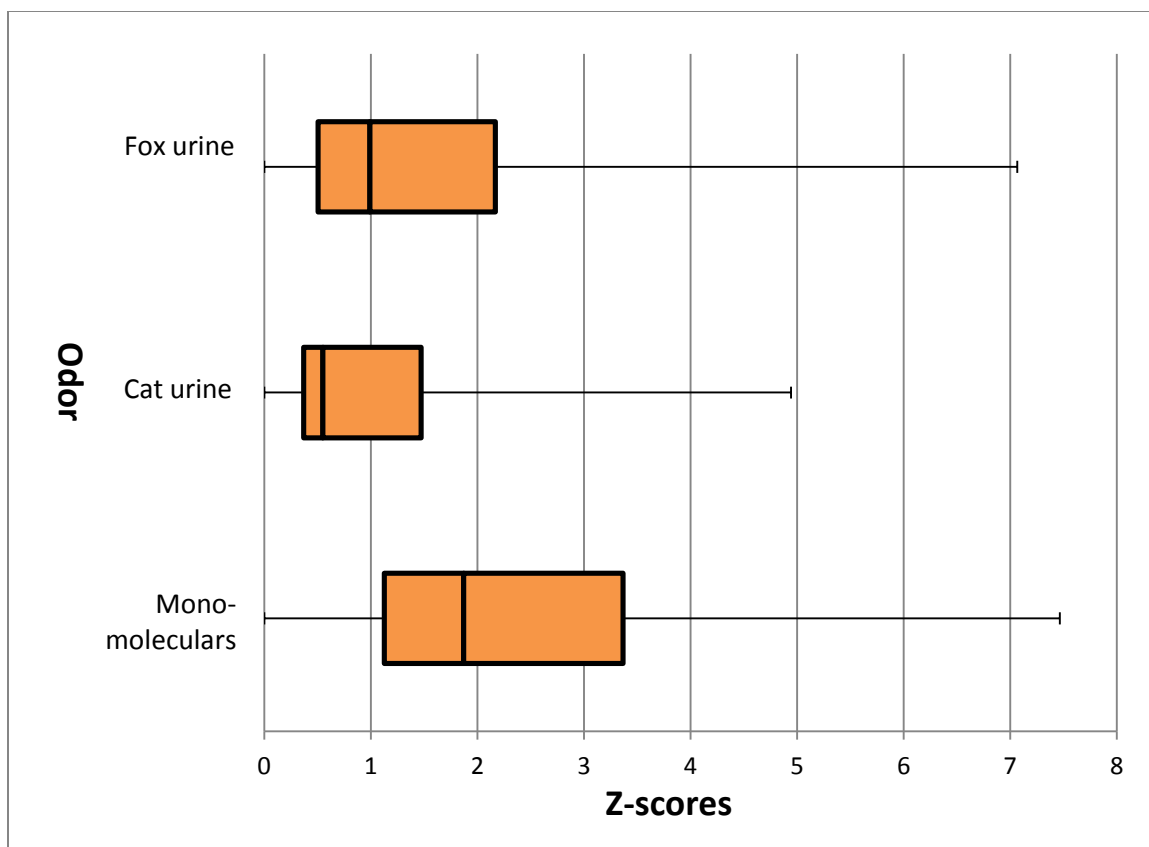
Figure 10: OT Responsivity to Pheromones and Monomolecular Odors Overall. No statistical significant differences detected. Data represented by z-scores and interquartile ranges. Error bars obtained by SEM. Fox urine ($n = 19$), cat urine ($n = 19$), monomolecular odors ($n = 74$).
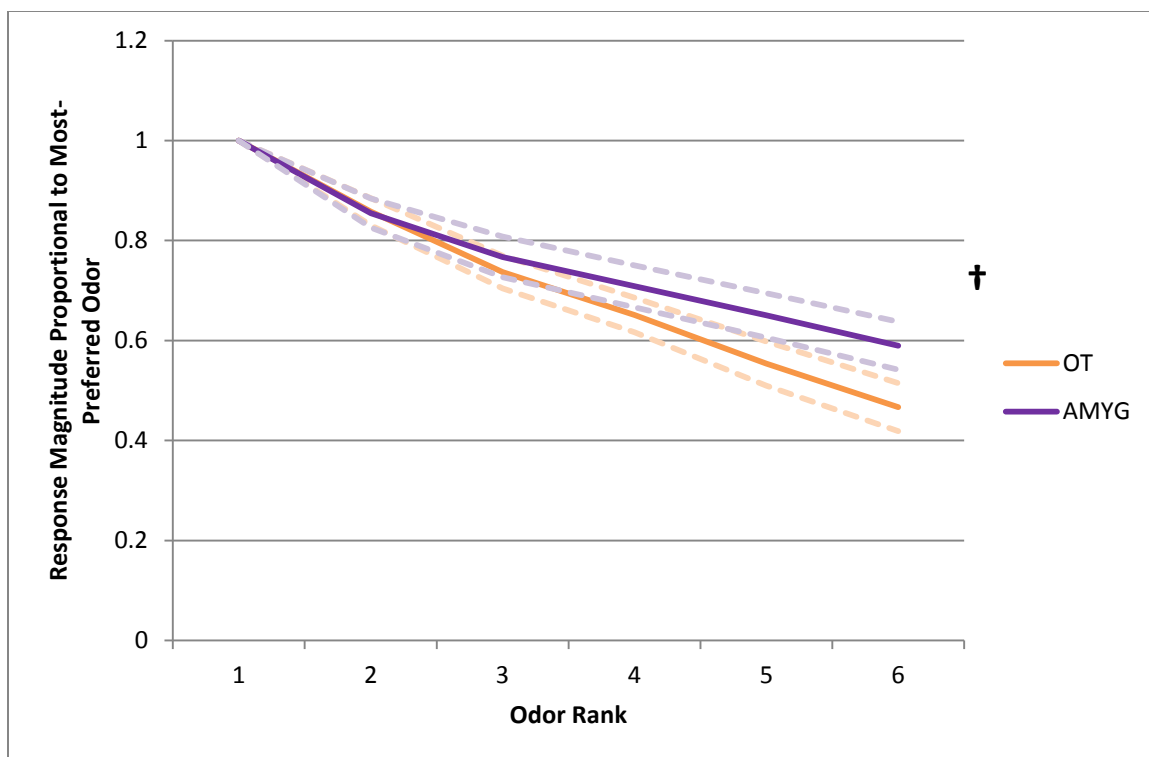
Figure 11: Tuning Breadth Comparison of OT and AMG. Responses to 6 monomolecular odors ranked according to magnitude of z-score. Z-scores converted into proportions. Z-scores averaged for each region, indicated by solid lines. Error bars calculated with SEM, indicated by dashed lines. No statistically significant differences detected. Trend at Rank 6, †$p = 0.072$.
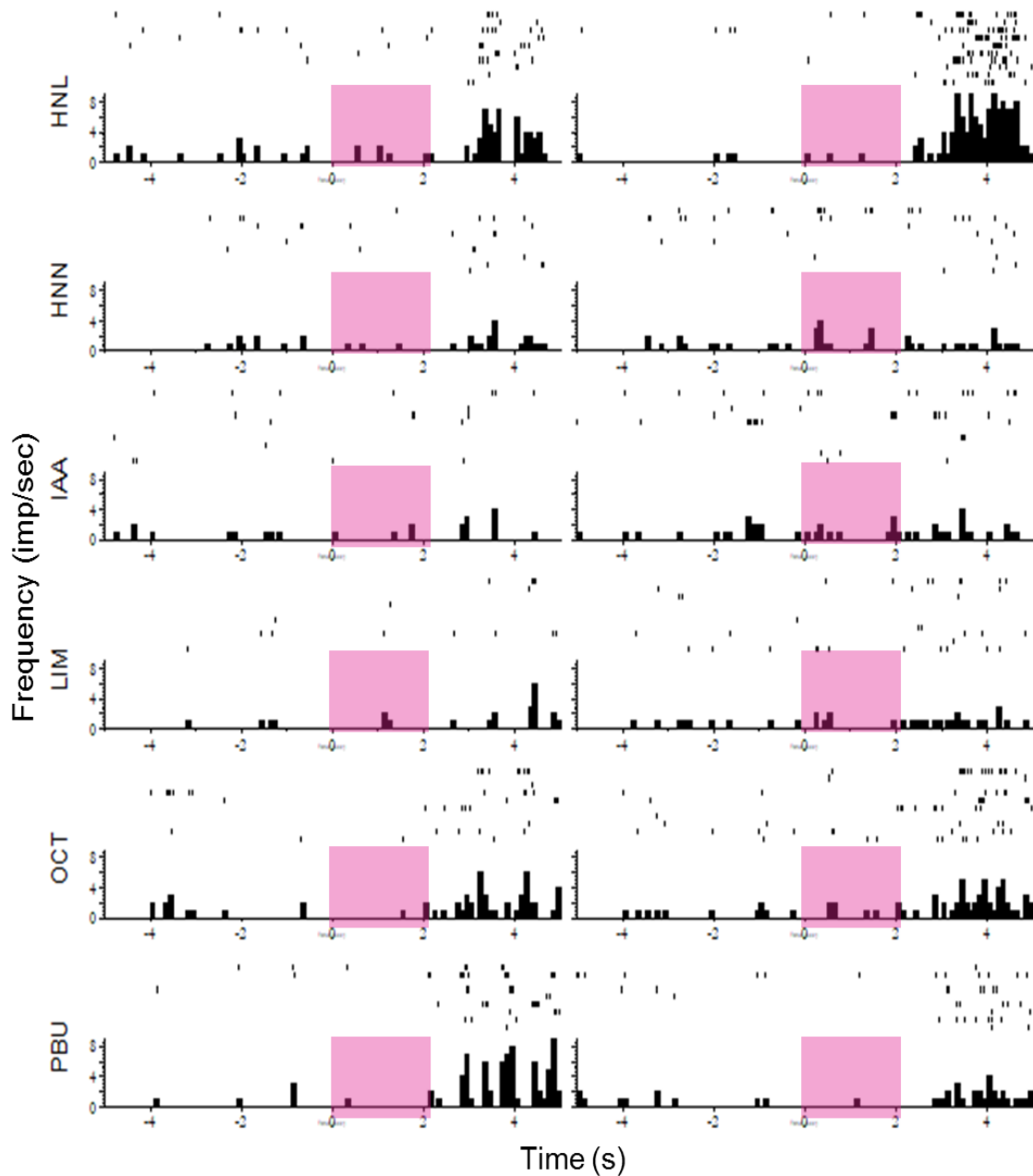
Figure 12: Correlated Tuning of Adjacent Cell Pairs. Isolated AMG neurons, cell A and cell D, exposed to 6 monomolecular odors (File Q24_4200). Number of rows in raster plots above indicate number of odor trials. Neuronal spikes are indicated by black vertical dashes. Histograms below average spike activity in the corresponding raster plot. Odor presentation (2 seconds) indicated by pink highlighted region.

Table 2: Correlated Tuning in OT and AMG Cell Pairs

		OT	AMYG
Total Cell Pair Comparisons		51	15
Correlated Cell Pairs	**Pairwise Comparisons**	4 / 51 (7.8%) $p = 0.081$	0 / 15 (0%)
	Subjective Histogram Evaluation	8 / 51 (15.7%)	1 / 15 (6.6%)

References

Alberts JR (1978) Huddling by rat pups: multisensory control of contact behavior, J Comp Physiol Psych 92:220-230.

Axel R (1995) The molecular logic of smell, Sci Am 273:154-159.

Bonhoeffer T, Grinvald A (1991) Iso-orientation domains in cat visual cortex are arranged in pinwheel-like patterns, Nature 353:429-431.

Boyd AM, Sturgill JF, Poo C, Isaacson JS (2012) Cortical feedback control of olfactory bulb circuits, Neuron 76:1161-1174.

Carriero G, Uva L, Gnatkovsky, De Curtis M (2008) Distribution of the olfactory fiber input into the olfactory tubercle of the in vitro isolated guinea pig brain, J Neurophysiol 101:1613-1619.

Doty R (2003) Handbook of olfaction and gustation, Marcel Dekker Inc., New York.

Fendt M, Endres T, Lowry CA, Apfelbach R, McGregor IS (2005) TMT-induced autonomic and behavioral changes and the neural basis of its processing, Neurosci Biobehav R 29:1145-1156.

Fitzgerald BJ, Richardson K, Wesson DW (2014) Olfactory tubercle stimulation alters odor preference behavior and recruits forebrain reward and motivational centers, Front Behav Neuro 8:1-9.

Franks KM, Isaacson JS (2006) Strong single-fiber sensory inputs to olfactory cortex: implications for olfactory coding, Neuron 49:357-363.

Gadizola MA, Tylicki KA, Christian DL, Wesson DW (2015) The olfactory tubercle encodes odor valence in behaving mice, JNeurosci 35:4515-4527.

Giessel AJ and Datta SR (2014) Olfactory maps, circuits, and computations, Curr Opin Neurobiol 2:120-132.

Haplern M (1987) The organization and function of the vomeronasal system. Annu Rev Neurosci, 10:325-362.

Iurilli G, Datta SR (2017) Population coding in an innately relevant olfactory area, Neuron 93:1180-1197.

Kang N, Wey A, Cherry JA, Baum MJ (2006) Laminated terminal fields in subdivisions of the medial amygdala receive direct inputs from the main and accessory olfactory bulbs of mice, unpublished findings.

Licht G, Meredith M (1987) Convergence of main and accessory olfactory pathways onto single neurons in the hamster amygdale, Exp Brain Res, 69:7-18.

Martinez-Marcos A (2008) On the organization of olfactory and vomeronasal cortices, Prog Neurobiol 87:21-30.

Merzenich MM, Knight PL, Roth GL (1974) Representation of cochlea within primary auditory cortex in the cat, J Neurophysiol 38:231-249.

Mori K, Shepherd GM (1994) Emerging principles of molecular signal processing by mitral/tufted cells in the olfactory bulb, Semin Cell Biol 5:65-74.

Mountcastle VB (1997) The columnar organization of the neocortex, Brain 120:701-722.

Pitkanen A, Savander V, LeDoux JE (1997) Organization of intra-amygdaloid circuitries in the rat: an emerging framework for understanding functions of the amygdala, Trends Neurosci 20:517-523.

Poo C, Isaacson JS (2009) Odor representations in olfactory cortex: "sparse" coding, global inhibition, and oscillations, Neuron 62:850-861.

Poo C, Isaacson JS (2011) A major role for intracortical circuits in the strength and tuning of odor-evoked excitation in olfactory cortex, Neuron 72:41-48.

Pro-Sistiaga P, Mohedano-Moriano A, Ubeda-Banon I, Arroyo-Jimenez MD, Marcos P, Artacho-Perula E, Crespo C, Insausti R, Martinez-Marcos A (2007) Convergence of olfactory and vomeronasal projections in the rat basal telencephalon, J Comp Neurol 504:346-362.

Raisman G (1972) An experimental study of the projection of the amygdala to the accessory olfactory bulb and its relationship to the concept of a dual olfactory system. Exp Brain Res, 14:395-408.

Reale RA, Imig TJ (1980) Tonotopic organization in auditory cortex of the cat, J Comp Neurol, 192:265-291.

Rennaker RL, Chen CF, Ruyle AM, Sloan AM, Wilson DA (2007) Spatial and temporal distribution of odorant-evoked activity in the piriform cortex, JNeurosci 27:1534-1542.

Root CM, Denny CA, Hen R, Axel R (2014) The participation of cortical amygdala in innate, odour-driven behavior, Nature 515:269-273.

Rosenblatt JS (1967) Nonhormonal basis of maternal behavior in the rat, Science 156:1512-1513.

Scalia F, Winans SS (1975) The differential projections of the olfactory bulb and accessory olfactory bulb in mammals, J Comp Neurol 161:31-55.

Schneider NY, Datiche F, Wilson DA, Gigot V, Thomas-Danguin T, Ferreira G, Coureaud G (2015) Brain processing of a configural vs elemental odor mixture in the newborn rabbit, Brain Struct Funct 21:2527-2539.

Sevelinges Y, Gervais R, Messaoudi B, Granjon L, Mouly A-M (2004) Olfactory fear conditioning induces field potential potentiation in rat olfactory cortex and amygdala, Learn Mem 11:761-769.

Shepherd GM, Chen WR, Greer CA (2004) Olfactory bulb: the synaptic organization of the brain, Oxford: Oxford Univ Press.

Shipley MR, Ennis M, Puche AC (2004) Olfactory system: the rat nervous system, Elsevier, San Diego.

Sosulski DL, Bloom ML, Cutforth T, Axel R, Datta SR (2011) Distinct representations of olfactory information in different cortical centres, Nature 472:213-219.

Stettler DD and Axel R (2009) Representations of odor in the piriform cortex, Neuron 63:854-864.

Tootell RB, Hadjikhani NK, Vanduffel W, Liu AK, Mendola JD, Sereno MI, Dale AM (1998) Functional analysis of primary visual cortex (V1) in humans, Proc Natl Acad Sci 95:811-817.

Tyll S, Budinger E, Noesselt T (2011) Thalamic influences on multisensory integration, Comm Integ Bio 4:378-381.

Wesson DW, Wilson DA (2010) Smelling sounds: olfactory-auditory sensory convergence in the olfactory tubercle, JNeurosci 30:3013-3021.

Wesson DW, Wilson DA (2011) Sniffing out the contributions of the olfactory tubercle to the sense of smell: hedonics, sensory integration, and more, Neurosci Biobehav Rev 3:655-668.

Wilson DA, Sullivan RM (2011) Cortical processing of odor objects, Neuron 72:506-519.

Winans SS, Scalia F (1970) Amygdaloid nucleus: new afferent input from the vomeronasal organ, Science 170:330-332.

Xu F, Shaefer M, Kida I, Schafer J, Liu N, Rothman DL, Hyder F, Restrepo D, Shepherd GM (2005) Simultaneous activation of mouse main and accessory olfactory bulbs by odors of pheromones. J Comp Neurol 489:491-500.

Xu W, Wilson DA (2012) Odor-evoked activity in the mouse lateral entorhinal cortex, Neuroscience 223:12-20.

Appendix: Abbreviations

A1: primary auditory cortex

AOB: accessory olfactory bulb

AMG: amygdala

CoA: cortical amygdala

HNL: 1-heptanal

HNN: 2-heptanone

IAA: isoamyl acetate

IQR: interquartile range

LIM: (R)-(+)-limonene

LOT: lateral olfactory tract

MeA: medial amygdala

MOB: main olfactory bulb

OCT: 1,7-octadiene

OT: olfactory tubercle

PBU: propyl buterate

Pir: piriform cortex

plCoA: posterolateral cortical amygdala

SD: standard deviation

TMT: trimethylthiazoline

V1: primary visual cortex